Decompaction of Cationic Gemini Surfactant-Induced DNA Condensates by β-Cyclodextrin or Anionic Surfactant

Meiwen Cao,[†] Manli Deng,[†] Xiao-Ling Wang,[‡] and Yilin Wang*,[†]

Key Laboratory of Colloid and Interface Science, Institute of Chemistry, and Beijing National Laboratory for Condensed Matter Physics, Institute of Physics, Chinese Academy of Sciences, Beijing 100190, People's Republic of China

Received: April 15, 2008; Revised Manuscript Received: August 18, 2008

Compaction of DNA by cationic gemini surfactant hexamethylene-1,6-bis-(dodecyldimethylammoniumbromide) ($C_{12}C_6C_{12}Br_2$) and the subsequent decompaction of the DNA−$C_{12}C_6C_{12}Br_2$ complexes by β-cyclodextrin (β-CD) or sodium dodecyl sulfate (SDS) have been studied by using ζ potential and particle size measurements, atomic force microscopy (AFM), isothermal titration microcalorimetry (ITC), and circular dichroism. The results show that $C_{12}C_6C_{12}Br_2$ can induce the collapse of DNA into densely packed bead-like structures with smaller size in an all-or-none manner, accompanied by the increase of ζ potential from highly negative values to highly positive values. In the decompaction of the DNA−$C_{12}C_6C_{12}Br_2$ complexes, β-CD and SDS exhibit different behaviors. For β-CD, the experimental results suggest that it can remove the outlayer hydrophobically bound $C_{12}C_6C_{12}Br_2$ molecules from the DNA−$C_{12}C_6C_{12}Br_2$ complexes by inclusion interaction, and the excess β-CD may attach on the complexes by forming inclusion complexes with the hydrocarbon chains of the electrostatically bound $C_{12}C_6C_{12}Br_2$ that cannot be removed. The increase of steric hindrance due to the attachment of β-CD molecules results in the decompaction of the DNA condensates though the true release of DNA cannot be attained. However, for SDS, the experimental results suggest that it can realize the decompaction and release of DNA from its complexes with $C_{12}C_6C_{12}Br_2$ due to both ion-pairing and hydrophobic interaction between SDS and $C_{12}C_6C_{12}Br_2$.

Introduction

DNA compaction and decompaction are two of the crucial steps in gene therapy. The compaction of DNA into small particles can protect DNA from degradation by nucleases as well as facilitate cell uptake,[1,2] while the decompaction and release of DNA inside the cells can recover the DNA properties so as to proceed to the following transcription.

The compaction of DNA by cationic surfactants has received much attention in recent years due to its potential use as a vehicle for gene delivery and gene transfection.[3−8] Surfactant-mediated DNA compaction usually exhibits a discrete first-order phase transition between an elongated coil state and a compacted globule state with increasing surfactant concentration.[5,7] Some early reports described DNA compaction as an all-or-none type transition over the whole molecular chain.[6,9] However, recent studies also confirmed that the intrachain segregation between the coils and globules could be generated as a thermodynamically stable state.[10−12] The cooperative binding of surfactant molecules on DNA chains, which is driven by both electrostatic and hydrophobic interactions, plays a crucial rule in the collapse of DNA molecules.

The decompaction of DNA condensates, which bears great importance as DNA compaction, has also attracted the interest of many researchers.[13,14] Mel'nikova and Dias et al.[15−17] and Bhattacharya et al.[18] have found that anionic surfactants could be used to unfold and release previously compacted DNA molecules by cationic surfactants. Bonincontro et al.[19,20] have studied the DNA adsorption and release from catanionic vesicles and attained an almost complete release of DNA by this method. Very recently, González-Pérez et al.[21] reported the successful decompaction of the DNA−cationic surfactant complexes by β-cyclodextrin (β-CD). Besides, monovalent salt,[22] synthetic polyacid,[5] neutral[23] and anionic liposomes,[24] and nonionic surfactant[25] have all shown the ability to dissociate DNA−surfactant complexes. Since these reagents used for DNA decompaction have quite different molecular natures, they should show different decompaction mechanisms.

In the present work, we have studied the compaction of DNA by a cationic gemini surfactant hexyl-α,ω-bis(dodecyldimethylammonium bromide) ($C_{12}C_6C_{12}Br_2$) and its decompaction by β-CD and an anionic surfactant sodium dodecyl sulfate (SDS). Gemini surfactant is chosen here due to its unique structure−activity correlations.[26−28] The results show that $C_{12}C_6C_{12}Br_2$ can successfully compact DNA into closely packed bead-like structures, and either β-CD or SDS can decompact the DNA−$C_{12}C_6C_{12}Br_2$ complexes. The results of the particle size, surface charge, morphology, and secondary structure of the complexes as well as the thermodynamic behaviors of the systems reveal that β-CD and SDS exhibit different mechanisms in decompacting the DNA−$C_{12}C_6C_{12}Br_2$ complexes. For β-CD, the experimental results suggest that it can form inclusion complexes with the hydrocarbon chains of the DNA-bound $C_{12}C_6C_{12}Br_2$ and increase steric hindrance inside the DNA−$C_{12}C_6C_{12}Br_2$ complexes, thus attaining the DNA decompaction. However, this method cannot truly release DNA from the complexes. Differently, for SDS, the experimental results suggest that it can release DNA from its complexes with $C_{12}C_6C_{12}Br_2$ due to both

* To whom the correspondence should be addressed. E-mail: yilinwang@iccas.ac.cn.
[†] Key Laboratory of Colloid and Interface Science, Institute of Chemistry.
[‡] Beijing National Laboratory for Condensed Matter Physics, Institute of Physics.

10.1021/jp803244f CCC: $40.75
Published on Web 10/08/2008

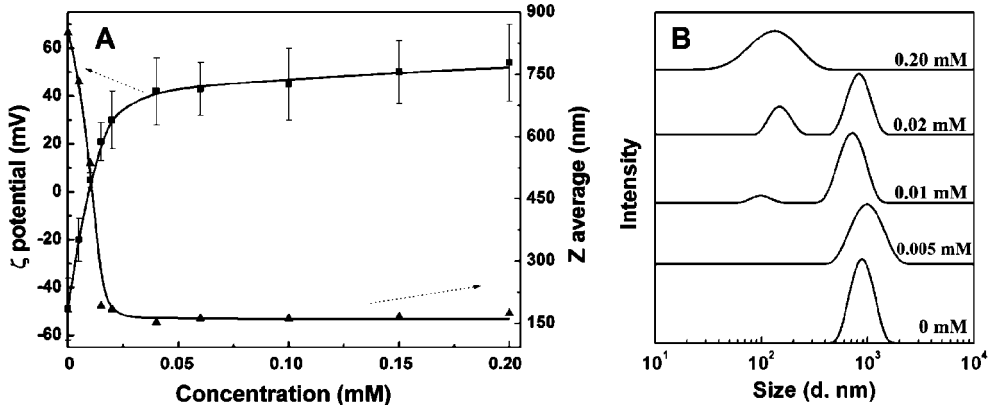

Figure 1. (A) Effect of $C_{12}C_6C_{12}Br_2$ concentration on (■) the ζ potential and (▲) the *Z* average of 2.5×10^{-8} mM DNA solution. Error bars indicate the deviation of the ζ potential, which is given by the equipment during measurements. (B) Typical intensity weighted distribution functions of the DNA solution in the absence and presence of $C_{12}C_6C_{12}Br_2$. $C_{12}C_6C_{12}Br_2$ concentrations are listed above the corresponding curves.

ion-pairing and hydrophobic interaction between SDS and $C_{12}C_6C_{12}Br_2$.

Experimental Section

Materials. λ-DNA ($M = 3.15 \times 10^7$, ca. 48.5 kbp) was purchased from New England BioLabs. Gemini surfactant $C_{12}C_6C_{12}Br_2$ was synthesized and purified according to the method of Menger and Littau.[29,30] The structure of $C_{12}C_6C_{12}Br_2$ was confirmed by ^{1}H NMR spectroscopy, and the purity was verified by elemental analysis and surface tension measurements. β-CD (>99%) and SDS (99.5%) were obtained from Acros and Sigma, respectively, and were used as received. Pure water (18 MΩ cm^{-1}) obtained from the Milli-Q system was used in all experiments.

ζ Potential and Particle Size Measurements. The ζ potential and the particle size measurements were performed at 20 °C, using a Malvern Zetasizer Nano-ZS instrument (ZEN3600, Malvern Instruments, Worcestershire, UK) equipped with a 4 mW He−Ne laser at a wavelength of 633 nm. A clear disposable capillary cell (DTS1060C) was used for both measurements. The cell was initially loaded with 1.0 mL of λ-DNA solution (2.5×10^{-8} mM, prepared with 10 mM Tris-buffer, pH 7.4). For the compaction of DNA by $C_{12}C_6C_{12}Br_2$, the concentrated $C_{12}C_6C_{12}Br_2$ solution of 10 mM was injected into the above λ-DNA solution in 0.5 μL per portion, giving the final $C_{12}C_6C_{12}Br_2$ concentration of about 0.2 mM. After each injection, the mixed solution was vortexed for about 30 s and then kept at 20 °C sufficiently long for the system to reach equilibrium, and then the ζ potential and the particle size measurements were performed. For the decompaction of the DNA−$C_{12}C_6C_{12}Br_2$ complexes, either the concentrated β-CD solution of 20 mM or SDS solution of 30 mM was injected into the above mixed solution of DNA and $C_{12}C_6C_{12}Br_2$ (2.5×10^{-8} mM λ-DNA, 0.2 mM $C_{12}C_6C_{12}Br_2$), in 5 μL per portion for β-CD and 2 μL per portion for SDS. After each injection, the system was also vortexed and equilibrated at 20 °C before measurements.

The ζ potentials were calculated from the mobility measured during an electrophoretic light-scattering (ELS) experiment, using the Hemholtz−Smoluchowski relationship. The particle size results are given in both size distribution and *Z* average. Size distribution is derived from a deconvolution of the measured intensity autocorrelation function of the sample accomplished by using a non-negatively constrained least-squares (NNLS) fitting algorithm. *Z* average is the intensity weighted mean hydrodynamic size of the ensemble collection of particles measured by dynamic light scattering (DLS). It is derived from a Cumulants analysis of the measured correlation curve. Though the Cumulants analysis cannot differentiate the different particle families, it does give information on the whole changing trend of the particle sizes in the system.

Isothermal Titration Microcalorimetry (ITC). The calorimeter used in this work is a TAM 2277-201 microcalorimeter (Thermometric AB, Järfälla, Sweden) with a 1 mL stainless steel sample cell. The cell was initially loaded with 0.5 mL of $C_{12}C_6C_{12}Br_2$ solution of 0.2 mM or the mixed solution of 2.5×10^{-8} mM DNA and 0.2 mM $C_{12}C_6C_{12}Br_2$. The concentrated β-CD solution (10 mM) or SDS solution (15 mM) was injected into the stirred sample cell in 3 or 2 μL per portion, using a 500-μL Hamilton syringe controlled by a Thermometric 612 Lund Pump. The system was stirred at 60 rpm with a gold propeller. The interval between two injections was kept sufficiently long for the system to reach equilibrium. Experiments were carried out at 298.15 ± 0.01 K.

Atomic Force Microscopy (AFM). A Multimode Nanoscope IIIa AFM (Digital Instruments, CA) was used for capturing AFM images of the complexes formed in different cases. For ambient imaging, a 10−15 μL sample solution was deposited onto a freshly cleaved piece of mica and allowed to incubate for 5−10 min. The sample was then dried with a gentle stream of pure nitrogen gas. The probes used were etched silicon probes with a nominal spring constant of 40 N/m (Digital Instruments, model RTESPW). All provided morphology images were recorded with a tapping mode at 512 × 512 pixel resolution and a scan speed of 1.0−1.8 Hz. They were shown in the height mode without any image processing except flattening. Analysis of the images was carried out with the Digital Instruments Nanoscope software (version 512r2).

Circular Dichroism. Circular dichroism spectra were recorded on a JASCO J-815 spectrophotometer at room temperature (20 ± 1 °C), using a 1.0-cm quartz cell. Scans were obtained in a range between 220 and 360 nm by taking points at 0.5 nm, with an integration time of 0.5 s. Typically, three spectra were averaged to improve the signal-to-noise ratio. The spectra were smoothed by using the noise reducing option in the software supplied by the vendor.

Results and Discussion

DNA Compaction by $C_{12}C_6C_{12}Br_2$. Figure 1A shows the effect of $C_{12}C_6C_{12}Br_2$ concentration on the ζ potential and the size of DNA. For DNA itself, the ζ potential is about −50 mV, similar to the result reported by Burckbuchler et al.,[31] and the

Z average is about 800 nm. However, the ζ potential increases sharply to about 40 mV with increasing $C_{12}C_6C_{12}Br_2$ concentration from 0 to beyond 0.025 mM, indicating the net charges on particles change from negative to positive. Simultaneously, the *Z* average decreases sharply to about 150 nm in this concentration range. Then, both the ζ potential and the *Z* average remain nearly constant with further increase of the $C_{12}C_6C_{12}Br_2$ concentration. The equilibrium of both the ζ potential and the *Z* average beyond the $C_{12}C_6C_{12}Br_2$ concentration of 0.025 mM indicates that DNA has been fully compacted, and the excess $C_{12}C_6C_{12}Br_2$ does not incorporate into the complexes further.

DNA compaction has been widely accepted as an all-or-none type transition over the whole molecular chain.[6,9] However, ζ potential and *Z* average results cannot reflect this stepwise transition well because they give the ensemble averages of ζ and *Z* values of different particle families. Figure 1B presents the typical intensity weighted distribution functions of the DNA solution in the absence and presence of $C_{12}C_6C_{12}Br_2$. As seen, the size distribution of DNA itself (0 mM $C_{12}C_6C_{12}Br_2$) presents only one peak with a mean hydrodynamic diameter of about 900 nm. This peak shows no great change at $C_{12}C_6C_{12}Br_2$ concentration lower than 0.005 mM. However, when increasing $C_{12}C_6C_{12}Br_2$ concentration to 0.01 mM, a second peak appears, which corresponds to a particle family with a smaller hydrodynamic diameter of around 120 nm. With further increasing $C_{12}C_6C_{12}Br_2$ concentration, this peak increases in amplitude while the ∼900 nm peak decreases. Then at the higher $C_{12}C_6C_{12}Br_2$ concentration of 0.20 mM, only the peak of 120 ± 30 nm presents. The original size of DNA, the size of the compacted DNA, as well as the size variation with increasng $C_{12}C_6C_{12}Br_2$ concentartion show high similarity to those of the cationic surfactant-induced DNA compaction observed by Dias et al.[32] The results reveal that a gradual change of the DNA size does not exist. Contrarily, the unchanged extended DNA coils and the compacted DNA molecules coexist in the system before all DNA molecules are compacted. This is the well-accepted all-or-none type transition.

AFM measurements were performed to gain insights into the DNA morphology change due to the $C_{12}C_6C_{12}Br_2$-induced compaction. The results are shown in Figure 2. As seen, DNA itself (Figure 2A) shows an elongated coiled structure with a large contour length. This state is ascribed to the high charge ratio and rigidity of the DNA chain. However, after interaction with $C_{12}C_6C_{12}Br_2$ (Figure 2B,C), DNA molecules form compacted structures. Clearly from the magnified images (the inset image), the compacted structures consist of multiple small bead-like structures, which are independent and do not fuse with each other. Moreover, we can find that all the compacted DNA structures at different concentrations of $C_{12}C_6C_{12}Br_2$ show approximately a uniform size. This result is consistent with the "all-or-none" transition and indicates that the compacted structures should be the result of the $C_{12}C_6C_{12}Br_2$-induced intrachain segregation of DNA. In conclusion, the AFM results confirm the successful compaction of DNA by $C_{12}C_6C_{12}Br_2$.

Previously, Yoshikawa and co-workers[26,27] found a "rings-on-a-string" structure in surfactant-induced DNA condensation by single-molecule fluorescence microscopy, and the "rings" were found to be torroids. In the present study, the compacted structure that may be called "beads-on-a-string" bears similarity to the above "rings-on-a-string" structure in shape. However, they exhibit great differences. The number of "beads" is much larger than the number of "rings", while the size of the "beads" is much smaller than the size of the "rings". Such differences indicate these beads should not be torroids. As known,

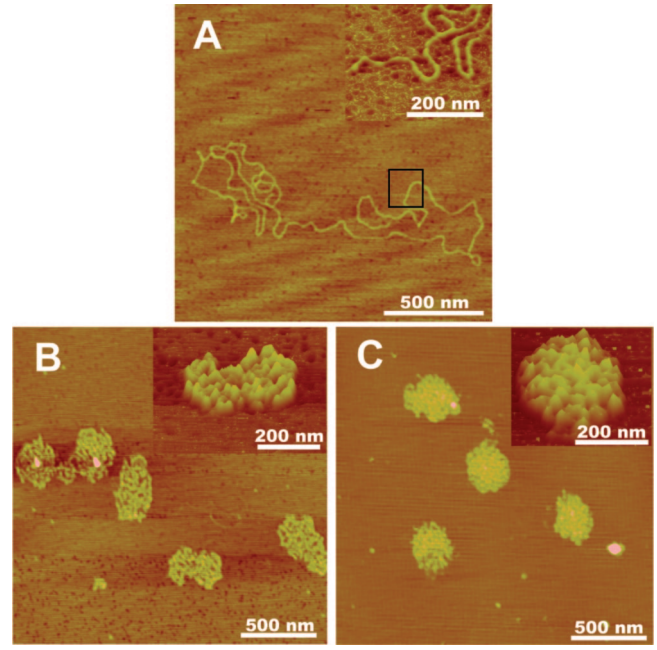

Figure 2. DNA morphologies obtained by AFM for (A) 2.5×10^{-8} mM DNA in Tris-buffer, (B) the mixed solution of 2.5×10^{-8} mM DNA with 0.01 mM $C_{12}C_6C_{12}Br_2$, and (C) the mixed solution of 2.5×10^{-8} mM DNA with 0.025 mM $C_{12}C_6C_{12}Br_2$.

electrostatically bound surfactant molecules on polyelectrolyte chains may form micelle-like aggregates due to hydrophobic interaction among their hydrocarbon chains.[33,34] Hence, we deduce that these bead-like structures may be formed by DNA chain wrapping around the micellar aggregates. In fact, such a proposition has been put forward by Wang et al. in a recent study.[34]

Decompaction of $C_{12}C_6C_{12}Br_2$-Induced DNA Condensates by β-CD and SDS. Figure 3 shows the effect of β-CD or SDS concentration on the *Z* average and the ζ potential of DNA−$C_{12}C_6C_{12}Br_2$ complexes. The *Z* average shows different variation with increasing β-CD or SDS concentration (Figure 3A). Without β-CD and SDS, the *Z* average of the DNA−$C_{12}C_6C_{12}Br_2$ complexes is 120 ± 20 nm. In the presence of β-CD, the *Z* average first shows small variation at the β-CD concentration lower than ∼0.4 mM. Then it starts to increase beyond this concentration and reaches the equilibrium value of about 800 nm at ∼1.2 mM β-CD. However, in the case of SDS, the SDS concentration where the *Z* average starts to increase is ∼0.2 mM, which is smaller than that of β-CD. And the increase of the *Z* average is much faster than that in the case of β-CD. The equilibrium *Z* average value is reached beyond the concentration of ∼0.3 mM. The increase of the *Z* average value in the two cases indicates that the DNA condensates have been decompacted by β-CD or SDS. Moreover, the decompaction process can also be concluded from the variation of size distribution of the samples with increasing β-CD or SDS concentration (Figure 3C,D). At lower concentrations, mainly a single peak presents and it broadens with increasing β-CD or SDS concentration. Then, beyond a certain critical concentration, which is about 0.50−0.60 mM for β-CD and ∼0.18 mM for SDS, the presence of two peaks can be observed in the curves. The peak with larger hydrodynamic diameter should be attributed to the decompacted DNA, while the peak with the smaller size probably indicates that not all the DNA condensates are decompacted at the used concentrations of β-CD and SDS.

The decompaction of DNA condensates by β-CD or SDS can also find support from the AFM results, as shown in Figure

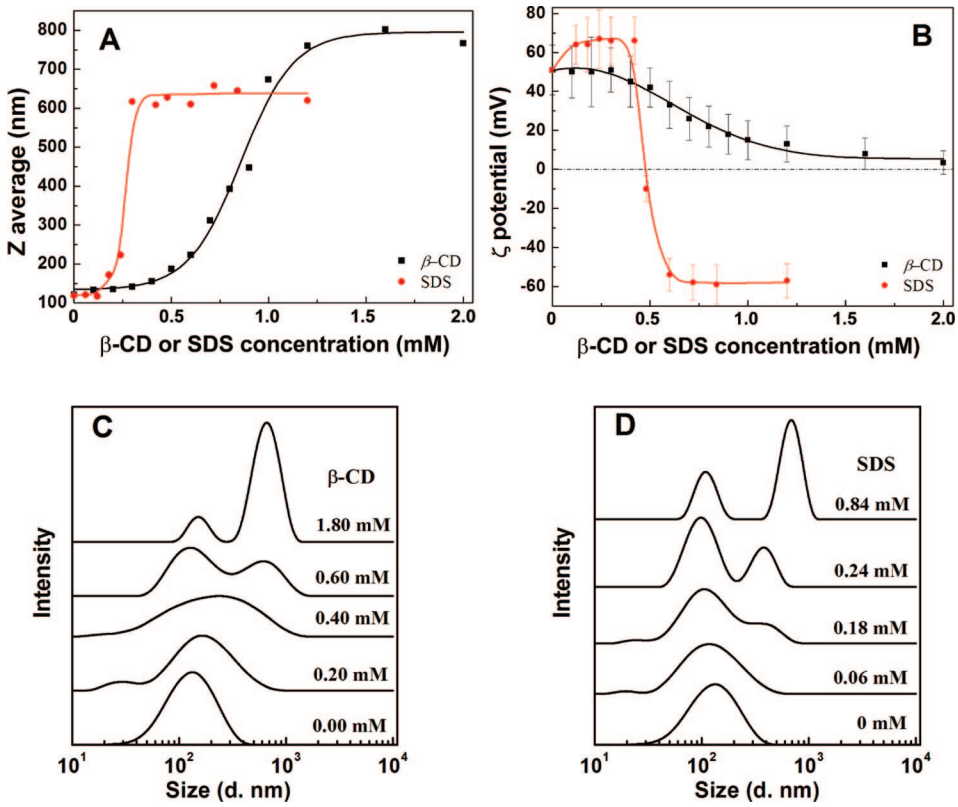

Figure 3. Effect of β-CD or SDS concentration on (A) the Z average and (B) the ζ potential of the mixed solution of 2.5×10^{-8} mM DNA and 0.2 mM $C_{12}C_6C_{12}Br_2$. Error bars indicate the deviation of the ζ potential, which is given by the equipment during measurements. Panels C and D show the typical intensity weighted distribution functions of the DNA/$C_{12}C_6C_{12}Br_2$ mixed solution in the absence and presence of β-CD or SDS, respectively. The concentrations of β-CD or SDS are listed above the corresponding curves.

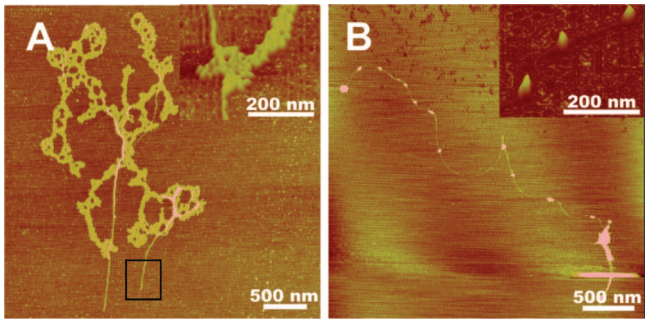

Figure 4. DNA morphologies obtained by AFM for the mixed solutions of (A) 2.5×10^{-8} mM DNA, 0.2 mM $C_{12}C_6C_{12}Br_2$, and 1.2 mM β-CD and (B) 2.5×10^{-8} mM DNA, 0.2 mM $C_{12}C_6C_{12}Br_2$, and 1.0 mM SDS.

4. The extended DNA chains can be found in both cases, even though their morphologies show some difference. In the case of β-CD (Figure 4A), the aggregates are relatively large and the DNA chain is imbedded in many tiny particles (the inset image), while in the case of SDS, the DNA presents separately and there are still some bead-like structures similar to those of the $C_{12}C_6C_{12}Br_2$-induced DNA condensates. We are not sure whether these bead-like structures after SDS treatment are the remaining compacted DNA segments or the aggregates formed by SDS and/or $C_{12}C_6C_{12}Br_2$ molecules on the DNA chain.

For the ζ potential (Figure 3B), the ζ potential of the mixed solution of 2.5×10^{-8} mM DNA and 0.2 mM $C_{12}C_6C_{12}Br_2$ is about 50 mV. However, the ζ potential exhibits different evolution with increasing concentration of β-CD or SDS. In the case of β-CD, the ζ potential almost does not change before the concentration of around 0.4 mM. Beyond 0.4 mM, the ζ potential decreases slowly with an increase of the β-CD concentration. Finally, the equilibrium value of nearly zero is reached at a β-CD concentration higher than 1.5 mM. Such a ζ potential variation indicates the particle surface changes from positively charged to nearly noncharged, while in the case of SDS, the ζ potential maintains the high value of 50−65 mV until the SDS concentration reaches about 0.4 mM. Then, the ζ potential shows a sharp decrease beyond 0.4 mM and quickly reaches the equilibrium value of about −60 mV at the SDS concentration of about 0.6 mM. In this course, the particle surface changes from positively charged to negatively charged.

In the case of β-CD, the ζ potential decreases from the large positive value to nearly zero, i.e., the density of positive charges on the surface of the DNA−$C_{12}C_6C_{12}Br_2$ complexes decreases gradually. As is well-known, β-CD is a cyclic oligosacharide in the shape of truncated cones with 7 units of α-glucopyranose. Its structure provides an external hydrophilic coat and an internal hydrophobic cavity.[31,35] These characteristics permit the formation of the inclusion complexes between β-CD and various molecular species including surfactants.[36−39] Guerrero-Martínez et al.[40,41] and Nilsson et al.[42] have revealed that β-CD can form 2:1 or 1:1 complexes with cationic ammonium gemini surfactants in which the surfactant tails may enter the hydrophobic cavity or interact with the external surface. In the present case, β-CD should also interact with $C_{12}C_6C_{12}Br_2$ and affect its interaction with DNA. Since the ζ potential only becomes nearly zero rather than negative, it is suggested that only a portion of the $C_{12}C_6C_{12}Br_2$ molecules can be removed from the DNA−$C_{12}C_6C_{12}Br_2$ complexes due to the interaction with β-CD. The possible situation is that the interaction can only remove the outlayer hydrophobically bound gemini molecules, but it is not strong enough to remove the electrostatically bound surfactant molecules. That is to say, the $C_{12}C_6C_{12}Br_2$ molecules

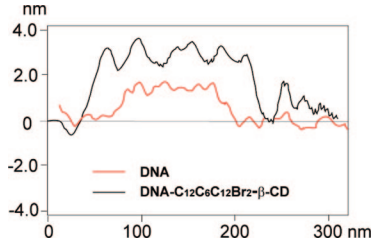

Figure 5. Section analysis of the AFM morphologies of DNA itself and the DNA−$C_{12}C_6C_{12}Br_2$−β-CD complexes. The segments analyzed are denoted by the black squares in Figure 2A and Figure 4A, respectively.

that neutralize the negative charges of DNA can be kept on DNA after interaction with enough β-CD. Excess β-CD molecules may attach on the surface of the DNA−$C_{12}C_6C_{12}Br_2$ complexes by forming inclusion complexes with the hydrophobic chains of the electrostatically bound $C_{12}C_6C_{12}Br_2$. Because β-CD is noncharged, the replacement of the outlayer positively charged $C_{12}C_6C_{12}Br_2$ with β-CD results in the decrease of the ζ potential from a large positive value to nearly zero. Moreover, attachment of sufficient β-CD may introduce great steric hindrance into the DNA intrachain aggregates and lead to the decompaction of them.

The attachment of β-CD on the surface of the DNA−$C_{12}C_6C_{12}Br_2$ complexes can also find support from the diameter variation of DNA molecules before and after treatment with $C_{12}C_6C_{12}Br_2$ and β-CD (Figure 5). The results reveal that both the height and the magnitude of surface fluctuation of DNA treated with $C_{12}C_6C_{12}Br_2$ and β-CD are larger than those of DNA itself. From this point of view, the tiny particles present in Figure 4A may be ascribed to the β-CD molecules attached on the DNA−$C_{12}C_6C_{12}Br_2$ complexes via inclusion interaction.

Another question is whether β-CD can bind directly on DNA to lower the ζ potential and enlarge its diameter? To answer this question, the ζ potential of the mixed solution of 2.5×10^{-8} mM DNA and 1.0 mM β-CD has been measured, which is about −40 mV. This value is only slightly less negative than that of DNA itself (about −50 mV). The result indicates that β-CD does not favor forming complexes with DNA, which is consistent with the observation of González-Pérez et al.[21] and Burckbuchler et al.[31]

In the case of SDS, the ζ potential of the DNA−$C_{12}C_6C_{12}Br_2$ complexes changes from a highly positive value (about 65 mV) to a highly negative value (about −60 mV) with increasing SDS concentration. This ζ potential variation indicates that cationic $C_{12}C_6C_{12}Br_2$ molecules are removed from the DNA surface due to both the strong electrostatic interaction between the oppositely charged SDS and $C_{12}C_6C_{12}Br_2$ and hydrophobic interaction among them. In this process, DNA regains its native negative charges, and the charge repulsion leads to the decompaction of DNA. In fact, Bhattacharya et al.[18] have demonstrated that DNA can be released from its complexes with cationic lipids by anionic amphiphiles because the combination of ion-pairing and hydrophobic interactions between cationic and anionic amphiphiles is stronger than the electrostatic force involved in the DNA−cationic lipid complexation.

Comparing the effect of β-CD with that of SDS, we can see that DNA itself, the DNA−$C_{12}C_6C_{12}Br_2$ complexes, and the DNA released by SDS−$C_{12}C_6C_{12}Br_2$ interaction all show large absolute ζ potentials, thus, they present separate adsorption morphologies due to electrostatic repulsion (Figures 2A,B and 4B). However, the DNA−$C_{12}C_6C_{12}Br_2$−β-CD complexes have the ζ potential of nearly zero, thus they exhibit higher propensity for aggregation and form webs (Figure 4A).

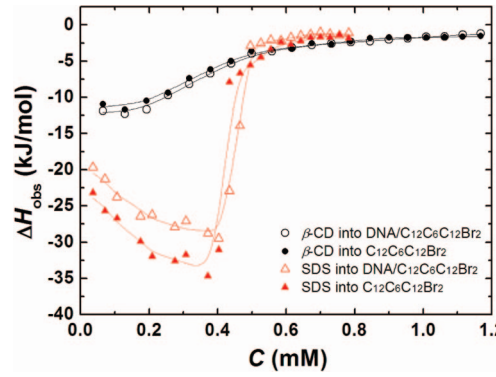

Figure 6. ITC curves for the titration of concentrated β-CD or SDS solution into 0.2 mM $C_{12}C_6C_{12}Br_2$ solution or the mixed solution of 2.5×10^{-8} mM DNA and 0.2 mM $C_{12}C_6C_{12}Br_2$.

To look further into the decompaction of the DNA−$C_{12}C_6C_{12}Br_2$ complexes induced by β-CD and SDS, we carried out the ITC measurements. The results are shown in Figure 6. Obviously, the observed enthalpy (ΔH_{obs}) of the titration of SDS into the DNA−$C_{12}C_6C_{12}Br_2$ mixed solution is much more exothermic than that of the titration of β-CD into the same DNA−$C_{12}C_6C_{12}Br_2$ solution at low SDS or β-CD concentrations. This difference in enthalpy change may be attributed to the different interactions in the two systems, i.e., hydrophobic interaction mainly involved in the case of β-CD and both electrostatic and hydrophobic interaction involved in the case of SDS.

For the titration of β-CD into $C_{12}C_6C_{12}Br_2$ solution and DNA−$C_{12}C_6C_{12}Br_2$ mixed solution, very similar calorimetric curves are obtained. This result indicates that the interaction between β-CD and DNA−$C_{12}C_6C_{12}Br_2$ complexes is virtually the same as that between β-CD and $C_{12}C_6C_{12}Br_2$. The gradual variation of ΔH_{obs} from the negative values to almost zero at the β-CD concentration range of 0 to about 0.4 mM should be caused by the formation of the inclusion complexes between β-CD and $C_{12}C_6C_{12}Br_2$. Beyond 0.4 mM, the nearly constant very small ΔH_{obs} indicates that mainly the dilution of β-CD is involved.

As to the titration of SDS into $C_{12}C_6C_{12}Br_2$ solution and DNA−$C_{12}C_6C_{12}Br_2$ mixed solution, though the ΔH_{obs} values show similar variation trend, the ΔH_{obs} values obviously differ at SDS concentrations lower than 0.4 mM. The ΔH_{obs} value for the titration of SDS into $C_{12}C_6C_{12}Br_2$ solution is about 5 kJ/mol more negative than that for the titration of SDS into DNA−$C_{12}C_6C_{12}Br_2$ mixed solution. For the titration of SDS into $C_{12}C_6C_{12}Br_2$, electrostatic ion-pairing and hydrophobic interaction between SDS and $C_{12}C_6C_{12}Br_2$ are the main interactions involved. For the titration of SDS into DNA−$C_{12}C_6C_{12}Br_2$ mixed solution, except for these two interactions, the broken electrostatic attraction between DNA and $C_{12}C_6C_{12}Br_2$ is also involved and should generate endothermic contribution to the enthalpy change of the process.

Generally, in the plots of ζ potential, Z average, or ΔH_{obs} as a function of β-CD or SDS concentration, the transition points are often observed around the concentration of 0.4 mM. This result is easy to understand if we notice that the concentration of $C_{12}C_6C_{12}Br_2$ is fixed at 0.2 mM in all the systems. That is to say, the hydrocarbon chains and the positive charges of $C_{12}C_6C_{12}Br_2$ are all 0.4 mM. Hence, stoichiometric amounts of β-CD or SDS are required to complete the interaction with $C_{12}C_6C_{12}Br_2$.

Maintenance of the original properties of DNA itself is crucial for its function in therapy. The double helix structure is an

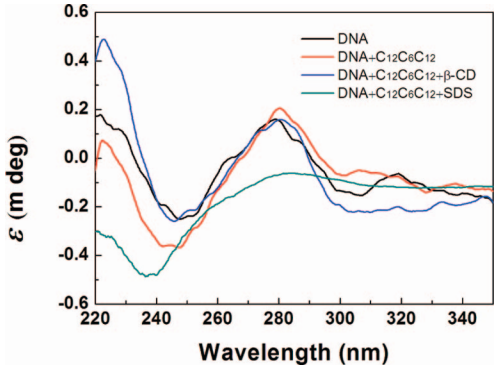

Figure 7. Circular dichroism spectra of DNA itself and after treatment with $C_{12}C_6C_{12}Br_2$, $C_{12}C_6C_{12}Br_2$ and β-CD, and $C_{12}C_6C_{12}Br_2$ and SDS.

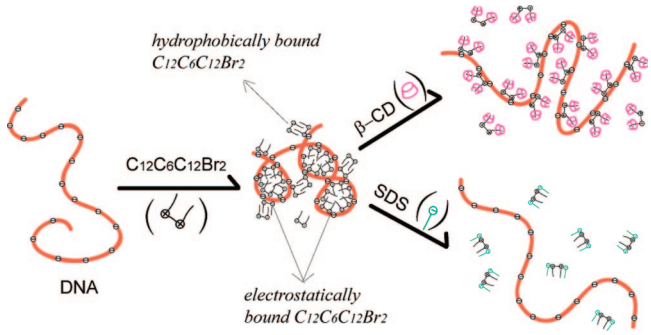

Figure 8. Illustration of the mechanisms of $C_{12}C_6C_{12}Br_2$-induced DNA compaction and decompaction of the DNA$-C_{12}C_6C_{12}Br_2$ complexes by β-CD or SDS.

important characteristic for DNA. To know the variation of the secondary structure of DNA during the above compaction and decompaction processes, the circular dichroism spectrum of native DNA and the spectra of DNA after different treatments are shown in Figure 7. On the whole, the curves all show a similar shape with a positive band at around 280 nm and a negative band between 240 and 250 nm. The results indicate that DNA maintains the B form in all cases, which is a typical native double-stranded conformation.[20] However, slight differences can also be found between the spectra of DNA after different treatments and DNA itself. Especially in the case of treatment with $C_{12}C_6C_{12}Br_2$ and then SDS, more obvious spectral changes present, including the slight shift of the negative band to lower wavelength and decrease of intensity of the positive band. The reason may be that the release of $C_{12}C_6C_{12}Br_2$ molecules from DNA surface through binding with SDS alters the double-helix conformation of DNA to a certain extent. Comparatively, the spectra of DNA after treatment with $C_{12}C_6C_{12}Br_2$ and after treatment with $C_{12}C_6C_{12}Br_2$ and then β-CD show little variation from the spectrum of DNA itself, indicating the DNA secondary structure has not been affected greatly.

Mechanisms of $C_{12}C_6C_{12}Br_2$-Induced DNA Compaction and Decompaction of the DNA$-C_{12}C_6C_{12}Br_2$ Complexes by β-CD or SDS. Taking all the above experimental results into account, we propose the following mechanisms for the compaction of DNA by $C_{12}C_6C_{12}Br_2$ and the decompaction of the DNA$-C_{12}C_6C_{12}Br_2$ complexes by β-CD or SDS, as shown in Figure 8.

For the compaction of DNA by $C_{12}C_6C_{12}Br_2$, $C_{12}C_6C_{12}Br_2$ molecules can bind on the oppositely charged DNA chain through electrostatic interaction, and these bound $C_{12}C_6C_{12}Br_2$ molecules may form micelle-like aggregates due to hydrophobic interaction among their hydrocarbon chains.[33,34] A micellar aggregate may act as a nucleation center and DNA will wrap around it to form a DNA spool, i.e., the bead-like structure.

In the decompaction of the DNA$-C_{12}C_6C_{12}Br_2$ complexes, β-CD and SDS exhibit different mechanisms. For the decompaction of the DNA$-C_{12}C_6C_{12}Br_2$ complexes by β-CD, β-CD can remove the outlayer hydrophobically bound $C_{12}C_6C_{12}Br_2$ molecules through inclusion interaction, and the excess β-CD molecules attach on the DNA$-C_{12}C_6C_{12}Br_2$ complexes by forming inclusion complexes with the hydrocarbon chains of the electrostatically bound $C_{12}C_6C_{12}Br_2$ molecules that cannot be removed from DNA. The increased steric hindrance caused by attachment of β-CD with larger size acts as the force to decompact the DNA condensates. This kind of decompaction cannot truly release DNA from its complexes with cationic surfactants. However, for the decompaction of the DNA$-C_{12}C_6C_{12}Br_2$ complexes by SDS, electrostatic ion-pairing and hydrophobic interaction between SDS and $C_{12}C_6C_{12}Br_2$ can remove both the hydrophobically bound $C_{12}C_6C_{12}Br_2$ and the electrostatically bound $C_{12}C_6C_{12}Br_2$ from DNA, which enables the recover of the DNA negative charges. In this case, the DNA condensates are decompacted by electrostatic repulsion between the negative charges on DNA. That is to say, the strong binding of SDS with $C_{12}C_6C_{12}Br_2$ can realize both decompaction and release of DNA.

Conclusions

The present study elucidates the compaction of DNA by cationic gemini surfactant $C_{12}C_6C_{12}Br_2$ and the subsequent decompaction of the DNA$-C_{12}C_6C_{12}Br_2$ complexes by β-CD or SDS. The results show that $C_{12}C_6C_{12}Br_2$ can induce the compaction of DNA into densely packed bead-like structures in an all-or-none manner. For the decompaction of the DNA$-C_{12}C_6C_{12}Br_2$ complexes, β-CD and SDS exhibit different mechanisms. For β-CD, the experimental results suggest that it can form inclusion complexes with the electrostatically bound $C_{12}C_6C_{12}Br_2$ molecules on DNA. The resulting steric hindrance among the intrachain aggregates can decompact the DNA condensates. However, DNA cannot be completely released from the complexes. On the other hand, for SDS, the experimental results suggest that it can strongly bind $C_{12}C_6C_{12}Br_2$ molecules through electrostatic ion-pairing and hydrophobic interaction and realize the release of $C_{12}C_6C_{12}Br_2$ molecules from DNA. This release recovers the DNA negative charges and the intrachain electrostatic repulsion decompacts the DNA condensates. Our present study provides further insights into the different mechanisms of DNA decompaction and may be helpful in the design and development of new reagents for gene therapy.

Acknowledgment..
We are grateful for financial support from the National Science Foundation of China (20633010, 20573123).

References and Notes

(1) Kichler, A.; Leborgne, C.; Coeytaux, E.; Danos, O. *J. Gene Med.* **2001**, *3*, 135–144.
(2) Zabner, J.; Fasbender, A. J.; Moninger, T.; Poellinger, K. A.; Welsh, M. J. *J. Biol. Chem.* **1995**, *270*, 18997–19007.
(3) Lasic, D. D. *Liposomes in gene delivery*; CRC Press: Boca Raton, FL, 1997.
(4) Templeton, N. S.; Lasic, D. D. *Mol. Biotechnol.* **1999**, *11*, 175–183.
(5) Mel'nikov, S. M.; Sergeyev, V. G.; Yoshikawa, K. *J. Am. Chem. Soc.* **1995**, *117*, 9951–9956.

(6) Mel'nikov, S. M.; Sergeyev, V. G.; Yoshikawa, K. *J. Am. Chem. Soc.* **1995**, *117*, 2401–2408.
(7) Marchetti, S.; Onori, G.; Cametti, C. *J. Phys. Chem. B* **2005**, *109*, 3676–3680.
(8) Matulis, D.; Rouzina, I.; Bloomfield, V. A. *J. Am. Chem. Soc.* **2002**, *124*, 7331–7342.
(9) Yoshikawa, K.; Takahashi, M.; Vasilevskaya, V. V.; Khokhlov, A. R. *Phys. Rev. Lett.* **1996**, *76*, 3029–3031.
(10) Takagi, S.; Tsumoto, K.; Yoshikawa, K. *J. Chem. Phys.* **2001**, *114*, 6942–6949.
(11) Yoshikawa, K.; Yoshikawa, Y.; Koyama, Y.; Kanbe, T. *J. Am. Chem. Soc.* **1997**, *119*, 6473–6477.
(12) Yoshikawa, Y.; Velichko, Y. S.; Ichiba, Y.; Yoshikawa, K. *Eur. J. Biochem.* **2001**, *268*, 2593–2599.
(13) Miguel, M. G.; Pais, A. A. C. C.; Dias, R. S.; Leal, C.; Rosa, M.; Lindman, B. *Colloids Surf. A* **2003**, *228*, 43–55.
(14) Lindman, B.; Mel'nikov, S.; Mel'nikova, Y.; Nylaner, T.; Eskilsson, K.; Miguel, M.; Dias, R.; Leal, C. *Prog. Colloid Polym. Sci.* **2002**, *120*, 52–58.
(15) Mel'nikov, S. M.; Dias, R.; Mel'nikova, Y. S.; Marques, E. F.; Miguel, M. G.; Lindman, B. *FEBS Lett.* **1999**, *453*, 113–118.
(16) Dias, R. S.; Lindman, B.; Miguel, M. G. *J. Phys. Chem. B* **2002**, *106*, 12608–12612.
(17) Dias, R. S.; Lindman, B.; Miguel, M. G. *J. Phys. Chem. B* **2002**, *106*, 12600–12607.
(18) Bhattacharya, S.; Mandal, S. S. *Biochemistry* **1998**, *37*, 7764–7777.
(19) Bonincontro, A.; La Mesa, C.; Proietti, C.; Risuleo, G. *Biomacromolecules* **2007**, *8*, 1824–1829.
(20) Bonincontro, A.; Falivene, M.; Mesa, C. L.; Risuleo, G.; Peña, M. R. *Langmuir* **2008**, *24*, 1973–1978.
(21) González-Pérez, A.; Dias, R. S.; Nylander, T.; Lindman, B. *Biomacromolecules* **2008**, *9*, 772–775.
(22) Mel'nikov, S. M.; Sergeyev, V. G.; Yoshikawa, K.; Takahashi, H.; Hatta, I. *J. Chem. Phys.* **1997**, *107*, 6917–6924.
(23) Mel'nikov, S. M.; Sergeyev, V. G.; Mel'nikova, Y. S.; Yoshikawa, K. *J. Chem. Soc., Faraday Trans.* **1997**, *93*, 283–288.
(24) Xu, Y.; Szoka, F., Jr. *Biochemistry* **1996**, *35*, 5616–5623.
(25) Dias, R. S.; Lindman, B.; Miguel, M. G. *Prog. Colloid Polym. Sci.* **2001**, *118*, 163–167.
(26) Miyazawa, N.; Sakaue, T.; Yoshikawa, K.; Zana, R. *J. Chem. Phys.* **2005**, *122*, 044902.
(27) Zinchenko, A. A.; Sergeyev, V. G.; Murata, S.; Yoshikawa, K. *J. Am. Chem. Soc.* **2003**, *125*, 4414–4415.
(28) Kirby, A. J.; Camilleri, P.; Engberts, J. B. F. N.; Feiters, M. C.; Nolte, R. J. M.; Söderman, O.; Bergsma, M.; Bell, P. C.; Fielden, M. L.; Rodríguez, C. L. G.; Guédat, P.; Kremer, A.; McGregor, C.; Perrin, C.; Ronsin, G.; van Eijk, M. C. P. *Angew. Chem., Int. Ed.* **2003**, *42*, 1448–1457.
(29) Menger, F. M.; Littau, C. A. *J. Am. Chem. Soc.* **1993**, *115*, 10083–10090.
(30) Zana, R.; Benrraou, M.; Rueff, R. *Langmuir* **1991**, *7*, 1072–1075.
(31) Burckbuchler, V.; Wintgens, V.; Lecomte, S.; Percot, A.; Leborgne, C.; Danos, O.; Kichler, A.; Amiel, C. *Biopolymers* **2006**, *81*, 360–370.
(32) Dias, R. S.; Innerlohinger, J.; Glatter, O.; Miguel, M. G.; Lindman, B. *J. Phys. Chem. B* **2005**, *109*, 10458–10463.
(33) Holmberg, K.; Jönsson, B.; Kronberg, B.; Lindman, B. *Surfactants and Polymers in Aqueous Solution*, 2nd ed.; Wiley: New York, 2003.
(34) Wang, C.; Li, X.; Wettig, S. D.; Badea, I.; Foldvari, M.; Verrall, R. E. *Phys. Chem. Chem. Phys.* **2007**, *9*, 1616–1628.
(35) Bender, M. L.; Komiyama, M. *Cyclodextrin Chemistry*; Springer-Verlag: Berlin, Germany, 1978.
(36) Valente, A. J. M.; Nilsson, M.; Söderman, O. *J. Colloid Interface Sci.* **2005**, *281*, 218–224.
(37) Cabaleiro-Lago, C.; Nilsson, M.; Söderman, O. *Langmuir* **2005**, *21*, 11637–11644.
(38) Piñeiro, Á.; Banquy, X.; Pérez-Casas, S.; Tovar, E.; García, A.; Villa, A.; Amigo, A.; Mark, A. E.; Costas, M. *J. Phys. Chem. B* **2007**, *111*, 4383–4392.
(39) Xing, H.; Lin, S. S.; Yan, P.; Xiao, J. X.; Chen, Y. M. *J. Phys. Chem. B* **2007**, *111*, 8089–8095.
(40) Guerrero-Martínez, A.; González-Gaitano, G.; Viñas, M. H.; Tardajos, G. *J. Phys. Chem. B* **2006**, *110*, 13819–13828.
(41) Guerrero-Martínez, A.; Domínguez-Gutiérrez, D.; Palafox, M. A.; Tardajos, G. *Chem. Phys. Lett.* **2007**, *446*, 92–97.
(42) Nilsson, M.; Cabaleiro-Lago, C.; Valente, A. J. M.; Söderman, O. *Langmuir* **2006**, *22*, 8663–8669.

JP803244F